

Ab Initio Study of the $X^- + \text{RCOY}$ Displacement Reactions with $R = \text{H}, \text{CH}_3$ and $X, Y = \text{Cl}, \text{Br}$

Chang Kon Kim,[†] Hong Guang Li,[†] Hai Whang Lee,[†] Chang Kook Sohn,[‡] Young I Chun,[‡] and Ikchoon Lee^{*,†}

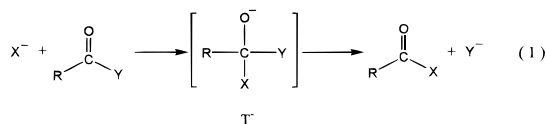
Department of Chemistry, Inha University, Incheon 402-751, Korea, and Department of Chemistry Education, Chonnam University, Kwangju 500-757, Korea

Received: December 1, 1999; In Final Form: February 21, 2000

The gas-phase acyl transfer reactions $X^- + \text{RCOY} \leftrightarrow \text{RCOX} + Y^-$ with $R = \text{H}, \text{CH}_3$ and $X, Y = \text{Cl}, \text{Br}$ have been investigated with MO theory at the G2(+)-MP2 level. Attempts have been made to locate two types of adducts, a tetrahedral adduct formed by an out-of-plane π -attack (π -adduct) and an adduct formed by an in-plane σ -attack (σ -adduct). In all cases, the σ -type adducts are nonexistent. Careful examination of the energies (ΔE) at the MP2/6-311+G** level shows that the transition structure region is very flat with a very low barrier for decomposition of the intermediate. This small barrier becomes inverted (i.e., the intermediate level is higher than the transition state) as the zero-point and thermal energy corrections are applied, which is eventually restored to the normal barrier ($\delta\Delta G = \Delta G_{\text{TS}} - \Delta G_{\text{Int}} \cong -0.9 \text{ kcal mol}^{-1}$) when entropy effect is accounted for. The π -adducts are stabilized mainly by the proximate second-order σ - σ^* type charge transfer interactions. The solvent effect evaluated in acetonitrile by the IPCM (isodensity polarizable continuum model) method raises activation energies, ΔG^\ddagger , by 9 ~ 13 kcal mol⁻¹, but the relative reactivity order in the gas phase, $-\Delta G^\ddagger(X, Y): (\text{Cl}, \text{Br}) > (\text{Cl}, \text{Cl}) > (\text{Br}, \text{Br}) > (\text{Br}, \text{Cl})$, is maintained in solution. The stepwise mechanism predicted in the gas phase and in solution is consistent with the experimental result.

Introduction

Considerable efforts have been made to determine the true nature, i.e., transition state (TS) or intermediate (Int), of the tetrahedral adduct, T^- , involved in the acyl transfer reactions,¹ eq 1. Theoretically, the gas-phase acyl transfer mechanism has been studied at various levels of MO theory.² Blake and Jorgensen^{2c} found double-well energy surfaces for the reactions of HCOCl (**I**) and CH_3COCl (**II**) with Cl^- at the MP2/6-31G**//HF/3-21G level. The adduct, T^- , is predicted to be a TS, and ion-dipole complexes are at the energy minima. Similarly, for the reactions of **II** + F^- and **II** + Cl^- , the adducts corresponded to the TSs at the 4-31G+p+p^{2d} level. In a recent high level ab initio investigation of the structural effects on the acyl transfer mechanism, we reported that the reactions of **I** and **II** with Cl^- proceed concertedly with the TS (T^-) located below the separated reactants.^{2e} The adduct, T^- , becomes an intermediate only when the acyl group, R, is a strong electron withdrawing group, e.g., $R = \text{CN}$ or NO_2 .



For the two reactions (**I** and **II** with $X = \text{Cl}$), we have collected the results reported at various theoretical levels in Table 1. The results of the uncorrelated MO theory in this table are seen to be unreliable, especially with respect to the identity (intermediate or TS) of the C_{2v} adduct. The first four entries in

TABLE 1: Activation Energies ($\Delta E^\ddagger = E(T^-) - E(\text{Reactant})$) for the Gas-Phase $\text{Cl}^- + \text{RCOCl}$ Reactions Calculated at Various Theoretical Levels

		$\text{Cl}^- + \text{RCOCl} \rightarrow [\text{Cl} - \text{RCOCl}]^- \rightarrow \text{RCOCl} + \text{Cl}^-$		
		ΔE^\ddagger ^a		
R	method	C_s ^b	C_{2v} ^c	ref
H	HF/3-21+G//HF/3-21+G	-7.1	-8.7	1c
	HF/6-31+G**//HF/3-21+G	4.8	3.3	1c
	MP2/6-31+G**//HF/3-21+G	-5.8	8.6	1c
	MP3/6-31+G**//HF/3-21+G	-1.4	10.2	1c
	HF/6-31+G**//HF/6-31+G*	6.0		1d
	MP2/6-31+G**//MP2/6-31+G*	-7.8 (-7.8) ^f	9.19 ^{e,f}	1d
	MP4/6-31+G**//MP2/6-31+G*	-8.3		1d
	MP2/6-311+G**//MP2/6-311+G**	-9.6 (-9.6) ^d		1d
	MP2/6-311+G**//MP2/6-311+G**	-9.6	8.2 ^e	f
	B3LYP/6-311+G**//B3LYP/6-311+G**	-10.7	2.8 ^e	f
CH_3	QCISD/6-311+G**//QCISD/6-311+G**	-6.0	11.0 ^e	f
	G2(+)/MP2//MP2/6-311+G**	-9.2	5.9 ^e	f
	HF/4-31++G//HF/4-31++G	7.6		1d
	HF/6-31+G**//HF/6-31+G*	4.7		1e
	MP2/6-31+G**//MP2/6-31+G*	-5.4		f
	MP4(SDTQ)/6-31+G**//MP2/6-31+G*	-6.2		1c
	G2(+)/MP2//MP2/6-311+G**	-6.6		f
	experimental	~ -7		18

^a ΔE^\ddagger in kcal mol⁻¹ relative to reactants. ^b The π -attack TS. ^c The σ -attack TS. ^d An intermediate with all positive Hessian eigenvalues. ^e Two negative eigenvalues in the Hessian matrix. ^f This work.

Table 1 were reported to correspond to transition states, whereas we found that the adducts are nonexistent.^{2e} We failed to locate an adduct with a C_{2v} symmetry (σ -attack) involved in an in-plane σ -attack S_N2 substitution at the MP2/6-311+G**//MP2/6-311+G** level. We obtained, in fact, two negative eigen-

* Corresponding author Fax: +82-32-8654855. E-mail: ilee@dragon.inha.ac.kr

[†] Inha University.

[‡] Chonnam University, Kwangju 500-757, Korea

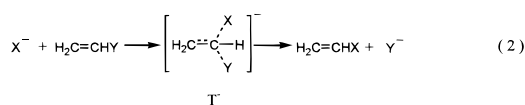
TABLE 2: Electronic Energies^a of Stationary Points Relative to the Separated Reactants for the Reaction $X^- + \text{RCOY} \leftrightarrow \text{RCOX} + Y^-$ at the MP2/6-311+G Level (in kcal mol⁻¹)**

R	reaction	Nu(X)	Lg(Y)	$\Delta E(\text{RC})^b$	adduct			
					type (sym)	$\Delta E^{\ddagger}(\text{T}^-)^c$	$\Delta E^{\circ}(\text{P})^d$	
H	1	Cl	Cl	-17.89	$\pi(C_s)$	-9.58 ₂ (-9.57 ₆) ^e	0	
				(8.31) ^f	$\sigma(C_{2v})$	8.18		
	2	Br	Br	-17.16	$\pi(C_s)$	-8.57 (-8.56) ^e	0	
				(8.59) ^f	$\sigma(C_{2v})$	4.29	0	
3	Cl	Br	Br	-20.21	$\pi(C_1)$	-12.71		
					$\sigma(C_1)$	0.01	-12.08	
Me	4	Br	Cl	-15.45	$\pi(C_1)$	-0.63		
					$\sigma(C_1)$	12.09	12.08	
	5	Cl	Cl	Cl	-13.37 (5.47) ^f	$\pi(C_s)$	-7.90 (-7.89) ^e	0
						$\pi(C_s)$	-6.84 ^g (-6.84) ^{e,g}	0
6	Br	Br	Br	-12.22 (5.38) ^f	$\pi(C_1)$	-11.17	-11.60	
					$\pi(C_1)$	0.43	11.60	

^a Not corrected for zero-point vibrational energy. ^b Reactant complex (RC) level, relative to the reactants. ^c Adduct (T⁻) level, relative to the reactants. ^d Product (P) level, relative to the reactants. ^e Values in parentheses are for transition state, which is confirmed by only one negative eigenvalue in the Hessian matrix. ^f The intrinsic barrier, ΔE_0^{\ddagger} , to the identity acyl transfer reaction. ^g The difference between the TS and intermediate is very small; $\delta\Delta E = \Delta E(\text{TS}) - \Delta E(\text{Int}) = 0.2 \times 10^{-4}$ kcal mol⁻¹.

values in the Hessian matrix indicating that it is neither a true TS nor an intermediate. The energy level of such a structure was much higher, by ca. 18 and 13 kcal mol⁻¹ than the true TS along the π -attack route, for the reactions of **I** and **II** with X = Cl, respectively.

On the other hand, in a recent G2(+)-MP2 level investigation³ in our laboratory of nucleophilic bimolecular substitutions at unactivated vinylic carbons ($\text{CH}_2 = \text{CHY}$, where Y = Cl) by anionic nucleophiles ($X^- = \text{OH}^-$, SH^- , Cl^- , or Br^-), eq 2, we found that the reactions proceed concertedly (T⁻ is a transition state) and an in-plane σ -attack with inversion of configuration ($\text{S}_{\text{N}}\sigma$ process) is preferred energetically by relatively weak nucleophiles ($X^- = \text{Cl}^-$ and Br^-), whereas an out-of-plane π -attack with retention of configuration ($\text{S}_{\text{N}}\pi$ process) is favored by stronger nucleophiles ($X^- = \text{OH}^-$ and SH^-). The second-order proximate σ - σ^* charge transfer term ($\Delta E_{\text{CT}} = \Sigma \Delta E_{\sigma-\sigma^*}^{(2)}$)⁴ is the major factor conducive to the energetic preference of the $\text{S}_{\text{N}}\pi$ processes for OH^- and SH^- , while the noncharge-transfer term (ΔE_{NCT})^{4a} involving strong electrostatic stabilization and low exclusion repulsion contributes predominantly to the energetic preference of the $\text{S}_{\text{N}}\sigma$ process over the $\text{S}_{\text{N}}\pi$ process for Cl^- and Br^- . Another important trend found is a reversal of the preferred paths in the substitution by Cl^- and Br^- from the $\text{S}_{\text{N}}\pi$ route at the lower correlated level of MP2/6-311+G**//MP2/6-311+G** to the $\text{S}_{\text{N}}\sigma$ route at the higher G2(+)-MP2 level.



In view of this surprising reversal of the preferred path depending on the computational level used, we extend in this work our investigation of the acyl transfer mechanism to the G2(+)-MP2 level⁵⁻⁷ for the acyl transfer reactions, eq 1, with R = H, CH₃ and X, Y = Cl, Br. We are interested to see whether such upgrading of the computational level can lead to a reversal of the energetic preference from the out-of-plane π -attack ($\text{S}_{\text{N}}\pi$ path) to the in-plane σ -attack ($\text{S}_{\text{N}}\sigma$ path) for the reactions of **I** and **II** with Cl^- . In addition, we aim to delve deeper into the problem of the nature of the adduct, T⁻, at the higher G2(+)-MP2 level of theory.

Calculation

Calculations were carried out using the *Gaussian 98* set of programs.⁸ All geometries of the reactants, products and stationary point structures were fully optimized. To determine whether the adduct (**I** + Cl^-) is an intermediate or TS, we have carried out characterizations of the adduct by harmonic vibrational analysis employing energy Hessians at four levels: B3LYP/6-311+G**, MP2/6-31+G*, MP2/6-311+G**, and QCISD/6-311+G**.⁹ The energies (ΔE) were corrected for zero-point vibrational energies (ZPE) with application of appropriate scaling factors and thermal energies (ΔH), and applied entropies to obtain free energy changes (ΔG) at 298 K. Energetics were discussed based on those at the G2(+)-MP2 level. The natural bond orbital (NBO) analyses^{4a} were performed to calculate the proximate σ - σ^* charge transfer energies. Solvent effect was calculated using the isodensity polarizable continuum model (IPCM) at the isodensity level of 0.0004 au¹⁰ in acetonitrile ($\epsilon = 36.64$).

Results and Discussion

Ion-Dipole Complexes. The energy profiles for all of the reactions have well-known double-well forms with two minima each corresponding to ion-dipole complexes. Characterization by vibrational frequency analysis shows that they are true minima with all positive eigenvalues in the Hessian matrix. The halide ion is located slightly off the C-H bond vector. In the case of CH_3COCl , this C-H bond is one of the two C-H which are trans to the carbonyl group (C=O). The loose H- Cl^- bond has relatively long distance ranging from 1.96 Å ($\text{BrCOH}-\text{Cl}^-$) to 2.48 Å ($\text{ClCOCH}_3-\text{Br}^-$). The well depths relative to the reactants (E_0) are summarized in Table 2. The reactant structure remains nearly unchanged in the reactant complex. The structures of reactants and reactant complexes are shown in the Supporting Information (S1). There is a slight stretching of the C-Y and C-H bonds and a small contraction of the C=O and C-C (**II**) bonds on going from reactant to ion-dipole complex. The MP2/6-311+G** complexation energies, $\Delta E(\text{RC})$ in Table 2 for $\text{HCOCl} + \text{Cl}^-$ (-17.9 kcal mol⁻¹), $\text{CH}_3\text{COCl} + \text{Cl}^-$ (-13.4 kcal mol⁻¹), and $\text{CH}_3\text{COBr} + \text{Br}^-$ (-12.2 kcal mol⁻¹) are quite reasonable in view of the experimental gas-phase $\Delta E(\text{RC})$ value of -12 ± 2 kcal mol⁻¹ for $\text{CH}_3\text{Cl} + \text{Cl}^-$ ¹¹ and -9.2 ± 0.5 kcal mol⁻¹ for $\text{CH}_3\text{Br} + \text{Br}^-$.¹² The carbonyl group in the acyl transfer reaction lowers the complexation

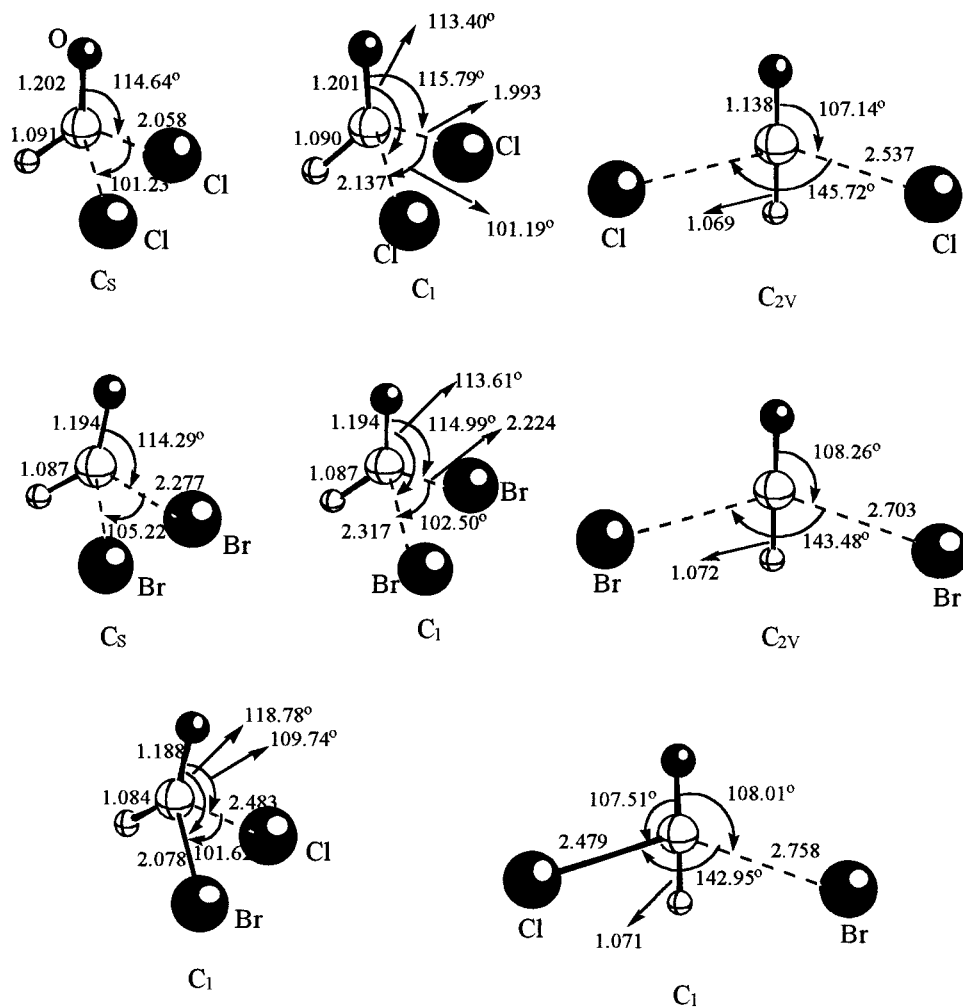


Figure 1. Structures (MP2/6-311+G**) of the π - and σ -adducts for the reactions of HCOY + X⁻.

energies by ca. 1 (X = Y = Cl) and 3 (X = Y = Br) kcal mol⁻¹ by strengthening the positive charge on the complexing H atom by electron withdrawal. The intrinsic barriers, ΔE_0^\ddagger defined as the barrier height from the reactant complex in an identity thermoneutral reaction,¹³ in Table 2 (MP2/6-311+G** level) for RCOCl + Cl⁻ reactions (8.3 and 5.5 kcal mol⁻¹ for R = H and CH₃, respectively) are somewhat lower than those at the MP2/6-31+G* level (9.9 and 7.5 kcal mol⁻¹ for R = H and CH₃, respectively).³ The ΔE_0^\ddagger values have been reported to be 13.3 kcal mol⁻¹ (experimental value: 13.2 ± 2.0 kcal mol⁻¹)¹⁴ for the gas-phase methyl transfer reaction of Cl⁻ + CH₃Cl and 11.2 kcal mol⁻¹ for Br⁻ + CH₃Br at the G2(+) level.¹⁵ Our gas-phase ΔE_0^\ddagger values for the acyl transfer reactions in Table 2 are considerably smaller than the ΔE_0^\ddagger values for these methyl transfer processes. This is most probably due to large stabilization of the TS for the acyl transfer by the proximate σ - σ^* type charge delocalization interactions including interactions involving $\pi_{C=O}^*$ orbital⁴ (Table 6), which are not present in the methyl transfer reactions.

Characterization of Adduct. Two types of adducts in the reaction of HCOCl + Cl⁻ have been considered: a tetrahedral adduct of C_s symmetry (T⁻) which is formed by an out-of-plane π -type attack (π -adduct) and an adduct of C_{2v} symmetry which is formed by an in-plane σ -type attack (σ -adduct). The structures optimized at the MP2/6-311+G** level are shown in Figure 1. Characterizations of the (π - and σ -) adducts by harmonic vibrational analysis were carried out at four different levels of theory (B3LYP/6-311+G**, MP2/6-31+G*, MP2/6-

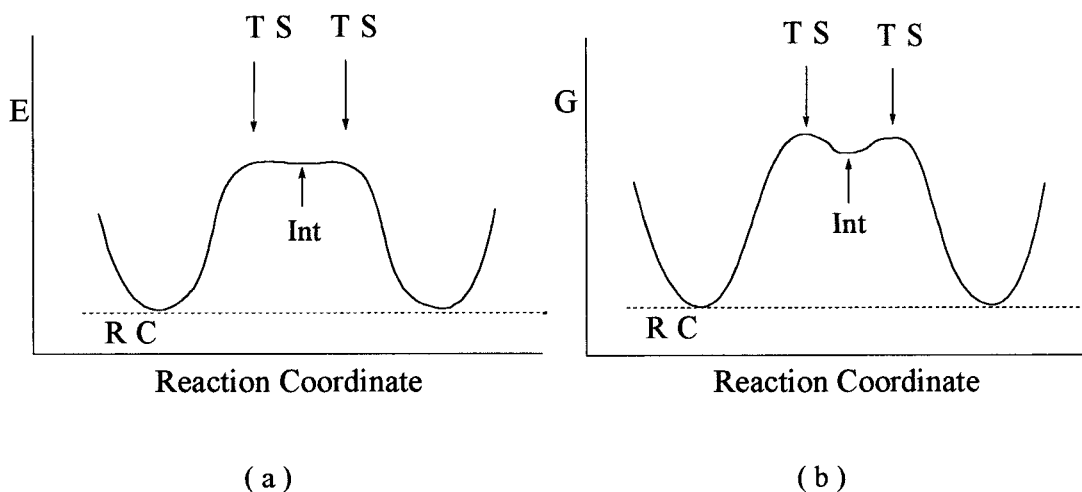
311+G**, QCISD/6-311+G** levels) as shown in Table 3. We note that at all levels of theory, the σ -adduct of C_{2v} symmetry has two negative eigenvalues in the Hessian matrix indicating that it is *neither a true TS nor an intermediate*. Such a σ -adduct may be considered as a transient structure in the inversion profile of tetrahedral adduct (T⁻) since it has an energy higher by 11 ~ 16 kcal mol⁻¹ than T⁻ (Table 3). This is in contrast to the energy profile obtained with lower level, uncorrelated energies. It has been shown that at the 3-21+G level the σ -adduct is planar and 1.6 kcal mol⁻¹ lower in energy than the π adduct (T⁻) with a slight barrier of 0.7 kcal mol⁻¹ between the two adducts (in fact, the two adducts were identified as transition states). The nonexistence of the σ -adduct is also in contrast to the energetic preference of the in-plane σ -attack (S_N σ process) over the out-of-plane π -attack (S_N π process) found in the nucleophilic vinylic substitutions of CH₂=CHCl by Cl⁻, eq 2 with X = Y = Cl.³

As to the identity of π -adduct (C_s symmetry), a true TS with only one negative eigenvalue in the Hessian matrix is predicted at all levels, except for an intermediate initially found at the MP2/6-311+G** level. We note in Table 3 that there are substantial differences in the activation energies, ΔE^\ddagger (and also in ΔG^\ddagger), depending on the level of theory used in the optimization. Comparison with the experimental ΔE^\ddagger value for CH₃COCl + Cl⁻ reaction in Table 1 indicates that our G2(+)-MP2/MP2/6-311+G** value gives the best theoretical estimate. For the HCOCl + Cl⁻ reaction, the MP2/6-311+G** ΔE^\ddagger (-9.6 kcal mol⁻¹) is quite close to the G2(+)-MP2 result (-9.2 kcal mol⁻¹). Compared with this, the B3LYP/6-311+G** value

TABLE 3: Characterization of the Adduct Formed in the Reaction of $\text{Cl}^- + \text{HCOCl}$ by Harmonic Vibrational Frequency Analysis at Various Level

computational level	adduct form ^a	symmetry	$\Delta E^{\ddagger a}$	ΔG^{\ddagger}	$\delta\Delta G^{\ddagger d}$	$d_{\text{C-Cl}}^e$
B3LYP/6-311+G**	π (i117 cm^{-1}) ^b	C_s	-10.47	-3.33	11.46	2.137
	σ (i758, i144 cm^{-1}) ^b	C_{2v}	1.20	8.13		2.547
MP2/6-31+G*	π (i97 cm^{-1}) ^b	C_s	-7.44	-0.18	14.65	2.101
	σ (i762, i120 cm^{-1}) ^b	C_{2v}	7.55	14.47		2.550
MP2/6-311+G**	π (I) ^c , (TS, 55 cm^{-1}) ^b	C_s	-9.14	-2.82	16.25	2.058
	σ (i794, i128 cm^{-1}) ^b	C_{2v}	6.54	13.43		2.537
QCISD/6-311+G**	π (i167 cm^{-1}) ^b	C_s	-5.48	1.83	16.37	2.048
	σ (i751, i100 cm^{-1}) ^b	C_{2v}	7.65	14.54		2.552

^a Adduct may be a transition state, intermediate or transient structure. ΔE^{\ddagger} , corrected by scaled zero point vibrational energy. Scaling factors: B3LYP/6-311+G**: 0.9806; MP2/6-31+G*: 0.9670; MP2/6-311+G**: 0.9748; QCISD/6-311+G**: 0.9776. ^b The negative eigenvalue(s) in the Hessian matrix. ^c I, intermediate, confirmed by all positive eigenvalues in the Hessian matrix. ^d $\delta\Delta G^{\ddagger} = \Delta G^{\ddagger}(\sigma) - \Delta G^{\ddagger}(\pi)$. ^e The distance C-Cl in the adduct.

**Figure 2.** Schematic energy profiles for the identity $\text{HCOX} + \text{X}^-$ gas-phase exchange reactions ($\text{X} = \text{Cl}, \text{Br}$) specifically showing the change in the flat transition region from ΔE (a) to ΔG (b).

is lower by ~ 1 kcal mol⁻¹ while the QCISD value is higher by ~ 3 kcal mol⁻¹. A similar trend was noted with the ΔE^{\ddagger} values calculated at the MP2/6-311+G** ($\Delta E^{\ddagger} = -45.8$ kcal mol⁻¹) and QCISD/6-311+G** (ΔE^{\ddagger} is higher by ~ 4 kcal mol⁻¹) levels for $\text{HCOH} + \text{H}^-$ reaction.³ Thus, the density functional theory (B3LYP) seems to underestimate while the QCISD method tends to overestimate the activation barriers to the identity acyl transfer reactions.

Optimized geometries are, however, very similar at the two higher levels predicting two different identities; bond length of the C-Cl is 2.058 and 2.048 Å, respectively, at the MP2/6-311+G** (an intermediate is predicted with all positive eigenvalues in the Hessian matrix) and QCISD/6-311+G** levels (a TS is predicted with only one negative eigenvalue in the Hessian matrix). Through a careful search of the flat transition structure region at the MP2/6-311+G** level, however, we were able to locate a true TS with only one negative eigenvalue corresponding to a barrier to decomposition of the intermediate, Figure 2. The intrinsic reaction coordinate (IRC) calculation showed that the TS is located on the decomposition pathway of the intermediate to the reactant (or product). The G2(+)-MP2 energies (ΔE) of the two, i.e., the TS and intermediate, are practically indistinguishable, differing only by 5.6 calories (Figure 2). When we correct for the zero-point (ZPE) and thermal energies (ΔH), the relative energy levels get

inverted leading to an absurd result of a lower TS level than the intermediate. The higher vibrational energy for the intermediate raises the zero-point corrected electronic energy (ΔE_{ZPE}) and ΔH levels of the intermediate higher than those of the TS. The vibrational energy of the TS is lower than that of the intermediate mainly because an asymmetric stretching vibrational mode (45.12 cm^{-1}) of the intermediate becomes translated (with imaginary frequency of 55.18 icm^{-1}) along the reaction coordinate in the TS. Thus, there is one less vibrational mode for the TS ($3N - 7 = 8$ modes for the TS in contrast to $3N - 6 = 9$ modes for the intermediate for $N = 5$), and accordingly the vibrational contributions to the thermal energy and entropy for the lost vibrational mode are missing in the TS.

The relative energy levels become restored to normal ($\Delta G^{\ddagger} > \Delta G_{\text{Int}}$, Figure 2b) only when the entropy effect is accounted for. The lower vibrational energy for the TS due to one less vibrational mode compared to the intermediate leads to a larger positive $-\text{T}\Delta S$ value (due to a larger negative ΔS value) and results in the higher ΔG^{\ddagger} than ΔG_{Int} level, $\delta\Delta G = \Delta G^{\ddagger} - \Delta G_{\text{Int}} > 0$. The energy changes are $\delta\Delta E (= \Delta E_{\text{TS}} - \Delta E_{\text{Int}} = +0.01$ kcal mol⁻¹) \rightarrow $\delta\Delta E_{\text{ZPE}} (= -0.06$ kcal mol⁻¹) \rightarrow $\delta\Delta H (= -0.60$ kcal mol⁻¹) \rightarrow $\delta\Delta G (= +0.90$ kcal mol⁻¹) as summarized in Table 4. It is therefore concluded that the $\text{HCOCl} + \text{Cl}^-$ (and also reactions **2**, **5**, and **6**) reaction is near mechanistic borderline for a change from a stepwise to a

TABLE 4: Energetics at MP2/6-311+G** Level (in kcal mol⁻¹)

R	reaction	Nu(X)	Lg(Y)	adduct form	symmetry	ΔE	ΔE_{ZPE}^a	ΔH^c	$-\Delta S^c$	ΔG^c	ΔE°	ΔG°		
H	1	Cl	Cl	π	$C_s(\text{Int})$	-9.58 ₂	-9.14	-9.44	6.62	-2.82	(-2.40) ^b	0	0	(0) ^b
					$C_1(\text{TS})$	-9.57 ₆	-9.20	-10.04	8.12	-1.92	(-1.60)	0	0	(0)
	2	Br	Br	π	C_{2v}	8.18	6.54	6.11	7.32	13.43	(11.14)	0	0	(0)
					$C_1(\text{Int})$	-8.57	-8.29	-8.43	6.03	-2.40	(-1.24)	0	0	(0)
	3	Cl	Br	π	$C_1(\text{TS})$	-8.56	-8.32	-9.03	7.93	-1.10	(0.02)	0	0	(0)
					C_{2v}	4.29	2.74	2.39	7.19	9.58	(9.64)	0	0	(0)
	4	Br	Cl	π	C_1	-12.71	-12.42	-13.05	7.72	-5.33	(-5.55)	-12.08	-11.60	(-9.64)
					C_1	0.01	-1.37	-1.82	6.97	5.15	(4.96)	-12.08	-11.60	(-9.64)
Me	5	Cl	Cl	π	C_1	-0.63	-0.77	-1.40	7.67	6.27	(4.09)	12.08	11.60	(9.64)
					C_1	12.09	10.28	-9.92	6.82	16.74	(14.59)	12.08	11.60	(9.64)
	6	Br	Br	π	$C_s(\text{Int})$	-7.90	-7.60	-7.87	7.15	-0.72	(0.58)	0	0	(0)
					$C_1(\text{TS})$	-7.89	-7.64	-8.46	8.82	0.36	(1.60)	0	0	(0)
	7	Cl	Br	π	C_1	-6.84 ^c	-6.59	-6.72	6.80	0.08	(1.91)	0	0	(0)
					C_1	-6.84 ^c	-6.62	-7.31	8.63	1.32	(3.31)	-11.60	-11.17	(-9.51)
	8	Br	Cl	π	C_1	-11.17	-10.77	-11.51	8.54	-2.97	(-2.30)	11.60	11.17	(9.51)

^a Zero point vibrational energy corrected value, zero point vibrational frequencies were scaled by 0.9748. ^b The values in parentheses are at the G2(+)-MP2 level. ^c The difference between the two is very small; $\delta\Delta E = \Delta E(\text{TS}) - \Delta E(\text{Int}) = 0.2 \text{ H } 10^{-4} \text{ kcal mol}^{-1}$.

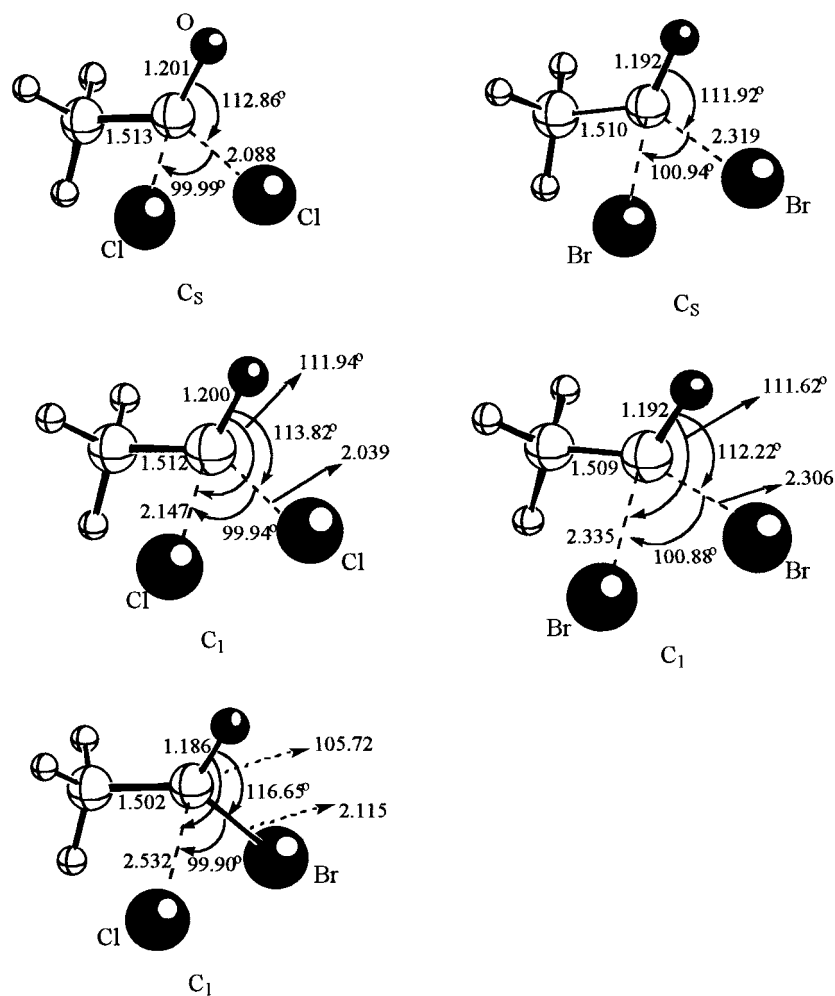


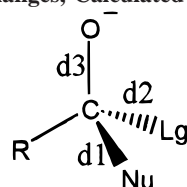
Figure 3. Structures (MP2/6-311+G**) of the π -adducts for the reactions of $\text{CH}_3\text{COY} + \text{X}^-$.

concerted mechanism. The reaction coordinate profile resembles that for the stepwise mechanism, but the intermediate barely exists because there is only an insignificant barrier for its breakdown (Figure 2). The structures in Figure 1 show that the intermediate has a C_s symmetry, whereas the TS has a C_1 symmetry but the structural difference is small.

An important caveat emerges from this study: It is quite dangerous to compare two electronic energy levels (ΔE) of very small energy difference, especially when they are corrected for zero-point (ΔE_{ZPE}) and thermal energies (ΔH), since an inver-

sion of the levels is possible unless entropy effects are accounted for, i.e., unless the comparison is made with the free energies, ΔG .

Similarly for other reactions, reaction numbers 2 ~ 8 in Tables 2 and 4, the σ -adducts were nonexistent. The energetically indistinguishable pair of π -adducts, a TS and an intermediate, are also found in the identity exchange reactions of $\text{RCOY} + \text{X}^-$ with $\text{R} = \text{CH}_3$, and $\text{X} = \text{Cl}$ and Br , reaction numbers 2, 5, and 6. We have given energetics for the π -adducts only for the reactions of CH_3COCl , reaction numbers 5 and 6 (C_1 and C_s symmetries), and 7 and 8 (C_1 symmetry) in Tables 2 and 4.

TABLE 5: Bond Lengths and Percent Bond Order Changes, Calculated at the MP2/6-311+G Level**

R	Nu (X)	Lg (Y)	variable	reactant	π -adduct (C_S or C_I)	σ -adduct (C_{2v} or C_1)	$\Delta d(\pi)$	$\Delta d(\sigma)$	$\% \Delta n^\pi(\pi)^a$	$\% \Delta n^\pi(\sigma)^a$
H	Cl	Cl	d1	∞	2.058	2.537	$-\infty$	$-\infty$	61.4	27.6
			d2	1.765	2.058	2.537	0.293	0.772	38.6	72.4
			d3	1.191	1.202	1.138	0.011	-0.053	3.6	19.3
	Br	Br	d1	∞	2.277	2.703	$-\infty$	$-\infty$	57.6	28.3
			d2	1.946	2.277	2.703	0.331	0.757	42.4	71.7
			d3	1.189	1.194	1.139	0.005	-0.050	1.7	18.1
	Cl	Br	d1	∞	2.483	2.479	$-\infty$	$-\infty$	30.2	30.4
			d2	1.946	2.078	2.758	0.132	0.812	19.7	74.2
			d3	1.189	1.188	1.139	-0.001	-0.050	-0.3	18.1
	Br	Cl	d1	∞	2.078	2.758	$-\infty$	$-\infty$	80.3	25.8
			d2	1.765	2.483	2.479	0.718	0.714	69.8	69.6
			d3	1.191	1.188	1.139	-0.003	-0.052	1.0	18.9
Me	Cl	Cl	d1	∞	2.088		$-\infty$		-61.4	
			d2	1.795	2.088		0.293		38.6	
			d3	1.193	1.201		0.008		2.6	
	Br	Br	d1	∞	2.319		$-\infty$		57.5	
			d2	1.987	2.319		0.332		42.5	
			d3	1.189	1.192		0.003		1.0	
	Cl	Br	d1	∞	2.532		$-\infty$		27.9	
			d2	1.987	2.115		0.128		19.2	
			d3	1.189	1.186		-0.003		1.0	
	Br	Cl	d1	∞	2.115		$-\infty$		80.8	
			d2	1.795	2.532		0.737		72.1	
			d3	1.193	1.186		-0.007		2.4	

^a For d1, d2, $\% \Delta n^\pi = [\exp(-r^\pi/a) - \exp(-r_R/a)] / [\exp(-r_P/a) - \exp(-r_R/a)] \times 100$, where r^π , r_R , and r_P are the bond length in the transition state (or intermediate) structure, reactant, and product, respectively, with $a = 0.6$, and for d3, $\% \Delta n^\pi = [\exp(-r^\pi/a) - \exp(-r_R/a)] / \exp(-r_P/a) \times 100$ with $a = 0.3$.

It is notable that our G2(+)/MP2 ΔE^\ddagger value ($-6.6 \text{ kcal mol}^{-1}$ in Table 1) for $\text{CH}_3\text{COCl} + \text{Cl}^-$ is similar to that at the MP4-(SDTQ)/6-31+G*/MP2/6-31+G* level ($-6.2 \text{ kcal mol}^{-1}$)^{2c} but closer to the experimental value of $\sim -7 \text{ kcal mol}^{-1}$. The TS structures for $\text{RCOY} + \text{X}^-$ reactions are presented in Figure 3.

Energetics. In the acyl transfer reactions, an important factor that determines whether the reactions proceed through a stable tetrahedral intermediate or through a tetrahedral TS is the $\sigma^*_{\text{C-Cl}}-\pi^*_{\text{C=O}}$ orbital mixing.^{2d,e} When the approaching nucleophile (X^-) forms a π -complex with the $\pi^*_{\text{C=O}}$ MO, the C-Cl bond begins to bend and this deformation in turn lowers the LUMO and leads to the $\sigma^*_{\text{C-Cl}}-\pi^*_{\text{C=O}}$ orbital mixing. If the two MOs are separated by a large energy gap, the mixing effect will be small and the nucleophile forms a tetrahedral intermediate through the π -approach. When, however, the energy gap is small the $\sigma^*_{\text{C-Cl}}-\pi^*_{\text{C=O}}$ orbital mixing becomes efficient and the $\sigma^*_{\text{C-Cl}}$ MO becomes a main component of the LUMO. Thus the π -attack of the nucleophile induces the C-Cl bond cleavage in a concerted process. The narrower the energy gap ($\Delta \epsilon^* = \epsilon_{\sigma^*} - \epsilon_{\pi^*}$) the greater the possibility of a concerted acyl transfer rather than a stepwise transfer through an intermediate. The energy gaps, $\Delta \epsilon^*$, calculated by the NBO method^{4a} with the HF/6-311+G** basis set (using MP2/6-311+G** geometries) were 3.9 and 3.1 eV for HCOCl and $\text{CH}_3\text{-COCl}$, respectively. They were even smaller for HCOBr (1.5 eV) and CH_3COBr (0.6 eV). These $\Delta \epsilon^*$ values are much smaller than those of the corresponding fluorides, 7.8 and 7.0 eV respectively, which are believed to react by a stepwise mechanism through an intermediate.^{2c} On account of the small $\sigma^*_{\text{C-Cl}}-\pi^*_{\text{C=O}}$ energy gap, the acyl transfer reactions of

chlorides and bromides are much more likely to proceed concertedly through a tetrahedral TS.

Bond lengths and percentage bond order changes¹⁶ [$\% \Delta n^\pi$ in eq 3 where r^π , r_R , and

$$\% \Delta n^\pi = \frac{[\exp(-r^\pi/a) - \exp(-r_R/a)]}{[\exp(-r_P/a) - \exp(-r_R/a)]} \times 100 \quad (3)$$

where r_P are the bond lengths in the TS (or intermediate), reactant, and product, respectively] are summarized in Table 5. We note that the π -adducts formed in the identity reactions ($\text{X} = \text{Y}$) are tight with a large extent of bond formation ($\sim 60\%$) and a small degree of bond cleavage ($\sim 40\%$), but the hypothetical σ -adducts are loose (with $\sim 30\%$ bond formation and $\sim 70\%$ bond cleavage). This trend is similar to that found in the nucleophilic vinylic substitution,³ eq 2. The identity reaction of $\text{X} = \text{Y} = \text{Cl}$ is in fact slightly tighter (61% and 39%) than that of Br (58% and 42%). The reaction of $\text{X} = \text{Cl}^-$ with HCOBr has an earliest TS with very small degree of bond formation (30%) and bond cleavage (20%) due partly to the exothermicity ($\Delta G^\circ = -11.2 \text{ kcal mol}^{-1}$) of the reaction. The reverse reaction ($\text{X} = \text{Br}$ with $\text{Y} = \text{Cl}$) has in contrast the latest TS due to endothermicity ($\Delta G^\ddagger = +11.2 \text{ kcal mol}^{-1}$). The substitution of $\text{R} = \text{CH}_3$ for $\text{R} = \text{H}$ leads to very little change in the $\% \Delta n^\pi$ values (Table 5). The tighter TS for the identity Cl^- exchange than for the identity Br^- reaction should be the major factor that leads to a lower ΔG^\ddagger value for $\text{RCOCl} + \text{Cl}^-$ ($\Delta G^\ddagger = -2.4$ and $0.6 \text{ kcal mol}^{-1}$ for $\text{R} = \text{H}$ and CH_3 , respectively) than for $\text{RCOBr} + \text{Br}^-$ ($\Delta G^\ddagger = -1.2$ and $1.9 \text{ kcal mol}^{-1}$ for $\text{R} = \text{H}$ and CH_3 , respectively); a stronger bond formed between C and Cl (bond energy for C-Cl is 81 kcal

TABLE 6: Second Order σ - σ^* Charge Transfer Energy Changes from Reactant (RCOY) to Adduct (T⁻) ($\delta\Delta E_{\sigma-\sigma^*}^{(2)} = \Sigma\Delta E_{\sigma-\sigma^*}^{(2)}(\text{T}^-) - \Sigma\Delta E_{\sigma-\sigma^*}^{(2)}(\text{R})$) and Electrostatic Interaction Energies ($\Sigma\Delta E_{\text{ES}}$) in the Adduct (in kcal mol⁻¹)

R	Nu(X)	Lg(Y)	adduct		$\delta\Delta E_{\sigma-\sigma^*}^{(2)}$	$\Sigma\Delta E_{\text{ES}}$
			form	symmetry		
H	Cl	Cl	π	C ₁	-212	14.4
			σ	C _{2v}	32	-69.6
	Br	Br	π	C ₁	-259	17.9
			σ	C _{2v}	41	-96.3
	Cl	Br	π	C ₁	-90	2.4
			σ	C ₁	32	-99.3
Br	Cl	π	C ₁	-86	2.4	
		σ	C ₁	36	-99.3	
Me	Cl	Cl	π	C ₁	-221	20.0
			σ	C ₁	-293	19.0
	Br	Br	π	C ₁	-94	5.6
			σ	C ₁	-94	5.6

TABLE 7: Deformation Energy,^a ΔE_{def} , Calculated at the MP2/6-311+G Level for RCOY in the Adduct Formation of RCOXY (in kcal mol⁻¹)**

R	X	Y	$\Delta E_{\text{def}}(\pi)$	$\Delta E_{\text{def}}(\sigma)$	$\delta\Delta E_{\text{def}}(\sigma-\pi)^b$
H	Cl	Cl	26.93	47.80	20.87
			24.68	41.45	16.77
	Br	Br	6.52	43.20	36.68
			57.84	45.85	-11.99
Me	Cl	Cl	26.98		
			24.35		
	Br	Br	7.62		
			54.34		

^a ΔE_{def} is the electronic energy required to deform the reactant (RCOY) to the structure in the TS or intermediate. ^b $\delta\Delta E_{\text{def}}(\sigma-\pi) = \Delta E_{\text{def}}(\sigma) - \Delta E_{\text{def}}(\pi)$.

mol⁻¹) in a tighter TS than C-Br (BE = 68 kcal mol⁻¹)¹⁷ should lead to a more stabilized TS for the Cl⁻ exchange reaction. This stabilization seems to contribute more than the proximate σ - σ^* type charge transfer interactions³ in Table 6 and the deformation energies in Table 7. Reference to these two tables reveals that the second-order σ - σ^* type charge transfer interaction energies (stabilization is less for X = Cl than Br) and deformation energies, ΔE_{def} ^{13,18} (destabilization is larger for X = Cl than Br) are in favor of the π -attack process by Br⁻ rather than by Cl⁻. The electrostatic energies in Table 6 are destabilizing for the π -adduct, but the difference between X = Cl and Br is small. Overall, the proximate σ - σ^* charge

TABLE 8: Solvation Free Energies in Acetonitrile ($\epsilon = 36.64$), Calculated by IPCM/MP2/6-311+G//MP2/6-311+G** with Isodensity Level of 0.0004 au**

R	Nu (X)	Lg (Y)	$\Delta G_s^{(R)a}$	$\Delta G_s^{(T)b}$	ΔG_{sol}^c	ΔG_{gas}^d	ΔG_{AN}^e	ΔG_{AN}^f	
H	Cl	Cl	(Int)	-62.19	-49.20	12.99	-2.40	10.59	0
			(TS)	-62.19	-49.35	12.84	-1.60	11.24	
	Br	Br	(Int)	-59.51	-46.82	12.69	-1.24	11.45	0
			(TS)	-59.51	-47.01	12.50	0.02	12.52	
	Cl	Br	(Int)	-62.19	-50.16	12.03	-5.55	6.48	-6.96
			(TS)	-59.51	-50.16	9.35	4.09	13.44	6.96
Me	Cl	Cl	(Int)	62.68	-49.50	13.18	0.58	13.76	0
			(TS)	-62.68	-49.48	13.20	1.60	14.80	
	Br	Br	(Int)	-59.98	-47.25	12.73	1.91	14.64	0
			(TS)	-59.98	-47.48	12.50	3.31	15.81	
	Cl	Br-	(Int)	62.66	-50.57	12.09	-2.30	9.79	-6.85
			(TS)	60.00	-50.57	9.43	7.21	16.64	6.85

^a The solvation free energy of reactant in acetonitrile, $\Delta G_s^{(R)} = \Delta E_s^{(R)} - E_g^{(R)}$, where $E_s^{(R)}$ is the energy of separated reactants in acetonitrile, and $E_g^{(R)}$ is the electronic energy of separated reactants in the gas phase. ^b The solvation free energy of T⁻ in acetonitrile, $\Delta G_s^{(T)} = E_s^{(T)} - E_g^{(T)}$, where $E_s^{(T)}$ is the energy of T⁻ in acetonitrile, and $E_g^{(T)}$ is the electronic energy of T⁻ in the gas phase. ^c $\Delta G_{\text{sol}}^c = \Delta G_s^{(T)} - \Delta G_s^{(R)}$. ^d The free energy difference between T⁻ and separated reactants in the gas phase, calculated at the G(2)MP2//MP2/6-311+G** level. ^e $\Delta G_{\text{AN}}^e = \Delta G_{\text{gas}}^c + \Delta G_{\text{sol}}^c$, the free energy difference between T⁻ and separated reactants in acetonitrile. ^f The reaction free energy in acetonitrile, $\Delta G_{\text{AN}}^f = \Delta G_{\text{gas}}^c + \Delta G_{\text{sol}}^c$, where $\Delta G_{\text{sol}}^c = \Delta G_s^{(P)} - \Delta G_s^{(R)}$.

transfer interactions are larger in the π -adduct than in the σ -adduct, but the electrostatic energies are in favor of the σ -adduct. This trend is also similar to that found in the nucleophilic vinylic substitution.³

Our G2(+)/MP2 result (Table 1) of ΔE^\ddagger (-6.6 kcal mol⁻¹) for CH₃COCl + Cl⁻ is in good agreement with that of the gas-phase experiment (~ -7 kcal mol⁻¹).¹⁹ The exothermicity of HCOBr + Cl⁻ (-9.6 kcal mol⁻¹) is also in good agreement with experiment (-9.9 kcal mol⁻¹).¹⁹ The ΔG^\ddagger values in Table 4 show that substitution of R = CH₃ for R = H raises the barrier by ca. 3 kcal mol⁻¹ uniformly, irrespective of the X and Y. This reflects an electron releasing effect of the CH₃ group, which leads to a looser TS (C-Cl distances are 2.137 and 2.147 Å for HCOCl and CH₃COCl, respectively). As discussed above, a tighter TS is more stable due to a stronger bond formation.

Solvent Effect. The solvation free energies calculated by the isodensity polarizable continuum model (IPCM)¹⁰ at the isodensity level of 0.0004 au are shown in Table 8. The activation free energies in acetonitrile, $\Delta G_{\text{AN}}^\ddagger$, are higher by 9 ~ 13 kcal mol⁻¹ than those in the gas phase, but the mechanism and the relative reactivity order in the gas phase, $-\Delta G^\ddagger(\text{X}, \text{Y})$, (Cl, Br) > (Cl, Cl) > (Br, Br) > (Br, Cl), for both R = H and CH₃ are maintained in solution. The exothermicity (or endothermicity) of the nonidentity reaction is reduced by ca. 2.6 kcal mol⁻¹, from -9.6 kcal mol⁻¹ in gas phase to -7.0 kcal mol⁻¹ in acetonitrile due to stronger solvation of Cl⁻ than of Br⁻. The barrier heights in acetonitrile, 6.5 ~ 16.6 kcal mol⁻¹, are well within the experimentally observable range at or near room temperature. The well depth, 0.7~1.0 kcal mol⁻¹, in acetonitrile is similar to or somewhat shallower than that in the gas phase (0.8~1.4 kcal mol⁻¹).

Experimentally, in aqueous solution the reactions of acetyl chloride (CH₃COCl) and methyl chloroformate (CH₃OCOCl) with basic amines (pK_a > 4) are reported to proceed by a rate-limiting nucleophilic attack, but the reactions with weakly basic (pK_a < 4) amines are predicted to react by a stepwise mechanism through a tetrahedral intermediate.²⁰ The reactions of methyl chloroformate (CH₃OCOCl) with pyridines are also known to show similar behavior in acetonitrile.²¹ Despite the neglect of the specific solvation component of the solvent effect in the IPCM method, the prediction of the same stepwise mechanism in acetonitrile as in the gas phase is rather surprising. The neglect of such solvent stabilization by specific solvation of the

intermediate, T^- , in the continuum model used in our calculation has relatively little effect on the mechanism. This is in line with the same mechanism predicted for methyl chloroformate in water and in acetonitrile.²⁰ The relatively low pK_a^o (≤ 4), at which the two nucleofuges present in the intermediate (amine and Cl^- ,²⁰ or in the present work X^- and Y^-) have the same leaving ability from the tetrahedral intermediate, T^\ddagger or T^- in solution, is an indication that the intermediate is of low stability or the well depth (Figure 2b) is relatively shallow even in solution. This is consistent with our conclusion that the gas-phase reactions have a very flat transition structure region where an intermediate well is so shallow that it has an insignificant barrier for its decomposition.

Summary

The gas-phase acyl transfer reactions $X^- + RCOY \rightarrow RCOX + Y^-$ with $R = H, CH_3$ and $X, Y = Cl, Br$ are found to proceed concertedly through tetrahedral transition states (π -adducts, T^-) formed by an out-of-plane π -attack. The σ -adduct formed by an in-plane σ -attack (σ -adduct) is neither an intermediate nor a transition state and does not correspond to a stationary point on the reaction coordinate in all cases.

The π -adduct in the identity reactions ($X = Y$) corresponds to either a transition state (at B3LYP/6-311+G**, MP2/6-311+G* and QCISD/6-311+G** levels) or an intermediate (at the MP2/6-311+G** level) depending on the level of theory used to characterize by harmonic vibrational analysis. Only through a careful examination of the energies ($\delta\Delta E = \Delta E_{TS} - \Delta E_{Int}$) at the MP2/6-311+G** level can a very flat transition structure region with an intermediate of insignificant barrier for its decomposition be located. This small barrier becomes inverted as the zero-point and thermal energy corrections are applied, which is eventually restored to the normal barrier when the entropy effect is accounted for: $\delta\Delta E$ ($\Delta E_{TS} - \Delta E_{Int} = +5.6$ kcal mol⁻¹) $\rightarrow \delta\Delta E_{ZPE}$ ($= -0.06$ kcal mol⁻¹) $\rightarrow \delta\Delta H$ ($= -0.60$ kcal mol⁻¹) $\rightarrow \delta\Delta G$ ($= +0.90$ kcal mol⁻¹). We conclude that the identity acyl transfer reactions, $RCOX + X^-$, with $R = H, CH_3$ and $X = Cl, Br$, are near mechanistic borderline for a change from a stepwise to a concerted mechanism. The reaction coordinate profiles resemble that for the stepwise mechanism, except that the intermediates barely exist because there are only insignificant barriers for their breakdown. The π -adducts are stabilized mainly by the proximate second-order σ - σ^* type charge transfer interactions. The solvent effect in acetonitrile by the IPCM method raises activation energies relative to the separated reactants, ΔG^\ddagger , by $9 \sim 13$ kcal mol⁻¹, but the mechanism and relative reactivity order in the gas phase, $-\Delta G^\ddagger$ -(X,Y):(Cl, Br) > (Cl, Cl) > (Br, Br) > (Br, Cl), is maintained in solution. The stepwise mechanism predicted in gas phase as well as in solution is consistent with the experimental result.

Acknowledgment. We thank Inha University for support of this work. This work was also supported by grant No. 1999-2-123-003-5 from the interdisciplinary Research program of the KOSEF.

Supporting Information Available: Structures (MP2/6-311+G**) of reactants and reactant complexes. This material is available free of charge via the Internet at <http://pubs.acs.org>.

References and Notes

(1) Experimental works. (i) In the gas phase: (a) Tiedemann, P. W.; Riveros, J. M. *J. Am. Chem. Soc.* **1974**, *96*, 185. (b) McMahon, T. B. *Can. J. Chem.* **1978**, *56*, 670. (c) Pau, J. K.; Kim, J. K.; Caserio, M. C. *J. Am. Chem. Soc.* **1978**, *100*, 3831. (d) Kim, J. K.; Caserio, M. C. *J. Am. Chem.*

Soc. **1981**, *103*, 2124. (e) Fukuda, E. K.; McIver, R. T., Jr. *J. Am. Chem. Soc.* **1979**, *101*, 2498. (f) Comisarow, M. *Can. J. Chem.* **1977**, *55*, 171. (g) Asubiojo, O. I.; Brauman, J. I. *J. Am. Chem. Soc.* **1979**, *101*, 3715. (h) Olmstead, W. N.; Brauman, J. I. *J. Am. Chem. Soc.* **1977**, *99*, 4219. (i) Bowie, J. H.; Williams, B. D. *Aust. J. Chem.* **1974**, *27*, 1923. (j) Bowie, J. H. *Acc. Chem. Res.* **1980**, *13*, 76. (k) McDonald, R. N.; Chowdhury, A. K. *J. Am. Chem. Soc.* **1983**, *105*, 7267. (l) McDonald, R. N.; Chowdhury, A. K. *J. Am. Chem. Soc.* **1983**, *105*, 198. (m) Larson, J. W.; McMahon, T. B. *J. Phys. Chem.* **1984**, *88*, 1083. (n) Klass, G.; Skeldon, J. C.; Bowie, J. H. *J. Chem. Soc., Perkin Trans. 2* **1983**, 1337. (o) Han, C. C.; Brauman, J. I. *J. Am. Chem. Soc.* **1990**, *112*, 7825. (p) Wilbur, J. L.; Brauman, J. I. *J. Am. Chem. Soc.* **1994**, *116*, 5939. (q) Tanner, S. D.; Mackay, G. I.; Bohme, D. K. *Can. J. Chem.* **1981**, *59*, 1615. (ii) In solution: (a) Bender, M. L. *Chem. Rev.* **1960**, *60*, 53. (b) Patai, S., Ed. *The Chemistry of Carbonyl Group*; Interscience: New York, 1966, 1970; Vols. 1, 2. (c) Jencks, W. P. *Acc. Chem. Res.* **1980**, *13*, 161. (d) Ba-Saif, S.; Luthra, A. K.; Williams, A. *J. Am. Chem. Soc.* **1987**, *109*, 6362. (e) Hengge, A. *J. Am. Chem. Soc.* **1992**, *114*, 6575. (f) Williams, A. *Chem. Soc. Rev.* **1994**, 93. (g) Williams, A. *Acc. Chem. Res.* **1989**, *22*, 387.

(2) (a) Burgi, H. B.; Lehn, J. M.; Wipff, G. *J. Am. Chem. Soc.* **1974**, *96*, 1956. (b) Burgi, H. B.; Dunitz, J. D.; Lehn, J. M.; Wipff, G. *Tetrahedron* **1974**, *30*, 1563. (c) Blake, J. F.; Jorgensen, W. L. *J. Am. Chem. Soc.* **1987**, *109*, 3856. (d) Yamabe, S.; Minato, T. *J. Org. Chem.* **1983**, *48*, 2972. (e) Lee, I.; Lee, D.; Kim, C. K. *J. Phys. Chem. A* **1997**, *101*, 879.

(3) Kim, C. K.; Hyun, G. H.; Kim, C. K.; Lee, I. *J. Am. Chem. Soc.*, **2000**, *122*, 2294.

(4) The σ - σ^* interactions include all types of second-order proximate charge transfer interactions involving n - σ^* , n - π^* , π - π^* , σ - π^* , π - σ^* , and σ - σ^* . (a) Reed, A. E.; Curtis, L. A.; Weinhold, F. *Chem. Rev.* **1988**, *88*, 899. (b) Epiotis, N. D.; Cherry, W. R.; Shaik, S.; Yates, R.; Bernardi, F. *Structural Theory of Organic Chemistry*; Springer-Verlag: Berlin, 1977, Part IV. (c) Musso, G. F.; Figari, G.; Magnasco, V. *J. Chem. Soc., Faraday Trans. 2* **1985**, *81*, 1243.

(5) The G2(+)/MP2 method is a modified G2(MP2)⁶ in which geometries are determined with an extra diffuse function (+) added. In the original G2 theory⁷ the energies are calculated with MP2(Full)/6-31G* geometries.

(6) Curtiss, L. A.; Raghavachari, K.; Pople, J. A. *J. Chem. Phys.* **1993**, *98*, 1293.

(7) Curtiss, L. A.; Raghavachari, K.; Trucks, G. W.; Pople, J. A. *J. Chem. Phys.* **1991**, *94*, 7221. (b) Curtiss, L. A.; Raghavachari, K.; Pople, J. A. *J. Chem. Phys.* **1995**, *103*, 4192.

(8) Frisch, M. J.; Trucks, G. W.; Schlegel, H. B.; Scuseria, G. E.; Robb, M. A.; Cheeseman, J. R.; Zakrzewski, V. G.; Montgomery, J. A., Jr.; Stratmann, R. E.; Burant, J. C.; Dapprich, S.; Millam, J. M.; Daniels, A. D.; Kudin, K. N.; Strain, M. C.; Farkas, O.; Tomasi, J.; Barone, V.; Cossi, M.; Cammi, R.; Mennucci, B.; Pomelli, C.; Adamo, C.; Clifford, S.; Ochterski, J.; Petersson, G. A.; Ayala, P. Y.; Cui, Q.; Morokuma, K.; Malick, D. K.; Rabuck, A. D.; Raghavachari, K.; Foresman, J. B.; Cioslowski, J.; Ortiz, J. V.; Stefanov, B. B.; Liu, G.; Liashenko, A.; Piskorz, P.; Komaromi, I.; Gomperts, R.; Martin, R. L.; Fox, D. J.; Keith, T.; Al-Laham, M. A.; Peng, C. Y.; Nanayakkara, A.; Gonzalez, C.; Challacombe, M.; Gill, P. M. W.; Johnson, B. G.; Chen, W.; Wong, M. W.; Andres, J. L.; Head-Gordon, M.; Replogle, E. S.; Pople, J. A. *Gaussian 98*, revision A.6; Gaussian, Inc.: Pittsburgh, PA, 1998.

(9) Foresman, J. B.; Frisch, A. *Exploring Chemistry with Electronic Structure Methods*; 2nd ed.; Gaussian Inc.: Pittsburgh, 1993.

(10) (a) Foresman, J.; Keith, T. A.; Wiberg, K. B.; Snoonian, J.; Frisch, M. J. *J. Phys. Chem. A* **1996**, *100*, 16098. (b) Wiberg, K. B.; Rablen, P. R.; Keith, T. A. *J. Am. Chem. Soc.* **1995**, *117*, 4261. (c) Rablen, P. R.; Pearlman, S. A.; Miller, D. A.; *J. Am. Chem. Soc.* **1999**, *121*, 227.

(11) Larson, J. W.; McMahon, T. B. *J. Am. Chem. Soc.* **1985**, *107*, 766.

(12) Deng, L.; Branchadell, V.; Ziegler, T. *J. Am. Chem. Soc.* **1994**, *116*, 10645.

(13) Shaik, S. S.; Schlegel, H. B.; Wolfe, S. *Theoretical Aspects of Physical Organic Chemistry. The S_N2 Mechanism*; Wiley: New York, 1992.

(14) Barlow, S. E.; Van Doren, J. M.; Bierbaum, V. M. *J. Am. Chem. Soc.* **1988**, *110*, 7240.

(15) Glukhovtsev, M. N.; Pross, A.; Schlegel, H. B.; Bach, R. D.; Radom, L. *J. Am. Chem. Soc.* **1996**, *118*, 11258.

(16) (a) Houk, K. N.; Gustabson, S. M.; Black, K. A. *J. Am. Chem. Soc.* **1992**, *114*, 8565. (b) Lee, I.; Kim, C. K.; Lee, B. S. *J. Comput. Chem.* **1995**, *16*, 1045. (c) Lee, J. K.; Kim, C. K.; Lee, I. *J. Phys. Chem. A* **1997**, *101*, 2893.

(17) Klumpp, G. W. *Reactivity in Organic Chemistry*; Wiley: New York, 1982.

(18) Mitchell, D. J.; Schlegel, H. B.; Shaik, S. S.; Wolfe, S. *Can. J. Chem.* **1985**, *63*, 1642.

(19) Asubiojo, O. I.; Brauman, J. I. *J. Am. Chem. Soc.* **1979**, *101*, 3715.

(20) (a) Bond, P. M.; Castro, E. A.; Moodie, R. B. *J. Chem. Soc., Perkin Trans. 2* **1976**, 68. (b) Palling, D. J.; Jencks, W. P. *J. Am. Chem. Soc.* **1984**, *106*, 4869.

(21) Koh, H. J.; Han, K. L.; Lee, H. W.; Lee, I. *J. Org. Chem.* **1998**, *63*, 9834.